Quark-model baryon-baryon interactions and their applications to few-body systems

Y. Fujiwara[1,a], Y. Suzuki[2], C. Nakamoto[3], M. Kohno[4], and K. Miyagawa[5]

[1] Department of Physics, Kyoto University, Kyoto 606-8502, Japan
[2] Department of Physics and Graduate School of Science and Technology, Niigata University, Niigata 950-2181
[3] Suzuka College of Technology, Suzuka 510-0294, Japan
[4] Physics Division, Kyushu Dental College, Kitakyushu 803-8580, Japan
[5] Department of Applied Physics, Okayama Science University, Okayama 700-0005, Japan

Abstract. The SU_6 quark-model baryon-baryon interaction by the Kyoto-Niigata group is reviewed with an emphasis on the unknown hyperon-nucleon interactions, especially, the ΞN interaction. With a newly developed framework to derive the baryon-octet (B_8) α interactions, we have examined $\Lambda\alpha$, $\Sigma\alpha$ and $\Xi\alpha$ central and LS potentials predicted by our models fss2 and FSS through the G-matrix calculations in symmetric nuclear matter. Our $\Lambda\alpha$ potential is comparable to the ones from the effective ΛN forces. The $\Lambda\alpha$ LS potential by FSS is consistent with the very small spin-orbit splitting of ${}^{9}_{\Lambda}$Be, experimentally observed. The $\Sigma\alpha$ potential is repulsive due to the very strong repulsion in the isospin $I = 3/2$ ${}^3S_1$ ΣN channel, which is induced from the Pauli principle at the quark level. A similar strong isospin dependence of the ΞN interaction implies that $\Xi\alpha$ central potential may not be strongly attractive, merely having an attraction of less than 5 MeV at the surface region. The $\Lambda(3N)$, $\Sigma(3N)$ and $\Xi(3N)$ central potentials are also discussed.

PACS. 13.75.Ev Hyperon-nucleon interactions – 21.60.Gx Cluster models – 21.80.+a Hypernuclei

1 Introduction

The QCD-inspired spin-flavor SU_6 quark model for the baryon-baryon interaction, proposed by the Kyoto-Niigata group, is a unified model for the full octet-baryons ($B_8 = N$, Λ, Σ and Ξ) [1,2]. In this model, the interaction Hamiltonian for quarks consists of the phenomenological confinement potential, the color Fermi-Breit interaction with explicit flavor-symmetry breaking (FSB), and effective meson-exchange potentials of scalar-, pseudoscalar- and vector-meson types [3]. The model parameters are determined to reproduce the properties of the nucleon-nucleon (NN) system and the low-energy cross section data for the hyperon-nucleon (YN) interactions. Once the quark-model Hamiltonian is assumed in the framework of the resonating-group method (RGM), the explicit evaluation of the spin-flavor factors leads to the stringent flavor dependence appearing in various interaction pieces. In this way we can utilize our rich knowledge of the NN interaction to minimize the ambiguity of model parameters, which is crucial since the present experimental data for the YN interaction are still very scarce. These quark-model interactions were used for the detailed study of few-baryon systems such as ^{3}H [4,5] and ${}^3_{\Lambda}$H [6], and also of some typical Λ-hypernuclei, ${}^{9}_{\Lambda}$Be [7,8] and ${}^{6}_{\Lambda\Lambda}$He [9], through a newly developed three-cluster Faddeev formalism [10,11] and G-matrix calculations [12–14]. We can now use these baryon-baryon interactions to calculate not only the $\Lambda\alpha$ interaction, but also $\Sigma\alpha$ and $\Xi\alpha$ interactions, assuming the harmonic-oscillator (h.o.) shell-model wave function for the α-cluster [15].

In this report, we first discuss an overview of the various B_8B_8 interactions predicted by our quark-model interaction. A current status of our understanding on the ΛN interaction is reviewed with respect to the S-wave and P-wave ΛN–ΣN coupling, where the one-pion exchange tensor force and the antisymmetric spin-orbit ($LS^{(-)}$) force, generated from the Fermi-Breit interaction, play a major role. A negligibly small ℓs splitting of ${}^{9}_{\Lambda}$Be excited states is discussed from the viewpoint of the $\Lambda\alpha$ interaction, which is derived from the G-matrix calculations. The strong repulsion in the $\Sigma N(I = 3/2)$ ${}^3S_1$ state yields a repulsive $\Sigma\alpha$ central potential, while attractive $\Sigma(3N)$ central potential in the spin 0 and isospin $T = 1/2$ state. A strong isospin dependence also appears in the ΞN interaction, which leads to the weakly attractive feature of the $\Xi\alpha$ central potential in the surface region.

[a] e-mail: yfujiwar@scphys.kyoto-u.ac.jp

Table 1. Characteristics of the quark-model B_8B_8 interactions, classified in the flavor SU_3 basis.

^1S, ^3P (P_{SF}-symmetric)		^3S, ^1P (P_{SF}-antisymmetric)	
(22)	attractive	(03)	strongly attractive
$(11)_s$	strongly repulsive	(30)	strongly repulsive
(00)	strongly attractive	$(11)_a$	weakly attractive

2 Characteristic features of the quark-model B_8B_8 interaction

Since the underlying quark-model Hamiltonian is approximately SU_3 scalar except for the strong one-pion exchange effect (due to the very small pion mass) and the FSB, it is essential to know the characteristic features of the B_8B_8 interaction classified in the SU_3 scheme. Table 1 shows these features which are mainly determined from the effect of the Pauli principle in the compact $(6q)$ structure and the dominated color-magnetic interaction in the quark-model Hamiltonian. In particular, the character of the SU_3 (00) state is strongly attractive, suggesting a possibility of the H-particle resonance in the strangeness $S = -2$ sector. On the other hand, our quark-model prediction for the $(11)_a$ state is weakly attractive both in the model fss2 and FSS. Since the $\Xi N(I = 0)$ $^3S_1$ state is composed of the pure $(11)_a$ state, it is urgent to determine this interaction from the experimental observables.

3 nα RGM by the quark-model G-matrix interaction

We have developed in Ref. [15] a general procedure to calculate $B_8\alpha$ Born kernel by using the nuclear-matter G-matrix of the quark-model baryon-baryon interaction. In this treatment, the nonlocality of the G-matrix and the center-of-mass motion between B_8 and α are explicitly treated in the cluster-model technique, under the assumption of the rigid $(0s)^4$ h.o. shell-model wave function of the α-cluster. We first applied this method to the $n\alpha$ RGM. Figure 1 shows the S-wave and P-wave $n\alpha$ phase shifts, predicted by fss2, for the neutron incident energies, E_n = 0 - 30 MeV. The G-matrix calculation in symmetric nuclear matter is carried out in the continuous choice for intermediate spectra, with constant G-matrix parameters, ω, K and $k_F = 1.20\,\mathrm{fm}^{-1}$. The h.o. size parameter $\nu = 0.257$ fm^{-2}, which corresponds to the matter root-mean-square (rms) radius of the α-particle, is used for the α-cluster. We find that the central and spin-orbit components of the $n\alpha$ interaction is reasonably reproduced without introducing any free parameters.

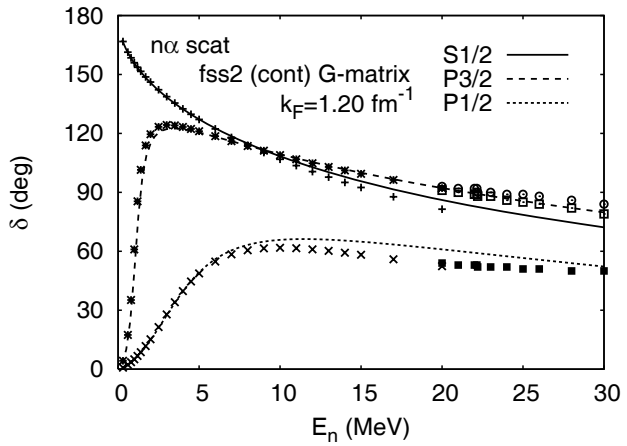

Fig. 1. $n\alpha$ RGM phase shifts predicted by the quark-model G-matrix interaction by fss2, compared with experiments.

4 ΛN interaction and Λα potential

The $^1S_0$ and $^3S_1$ phase shifts of the ΛN interaction are both attractive, but the relative strength is crucial to reproduce the hypertriton $^3_\Lambda$H, and the 0^+ and 1^+ states of $^4_\Lambda$H and $^4_\Lambda$He. The detailed Faddeev calculation using fss2 and FSS implies that the $^1S_0$ ΛN interaction is slightly more attractive than $^3S_1$ state [6]. Although the binding energy of the hypertriton in Ref. [6] is too large even for fss2, a small increase of the κ-meson mass cures this defect, yielding a result quite similar to the Nijmegen NSC89. However, enough attraction in the $^3S_1$ ΛN interaction is necessary to obtain the 1^+ states of the $^4_\Lambda$H and $^4_\Lambda$He systems in the right energy position.

Figure 2 shows the $\Lambda\alpha$ potentials derived from the α cluster folding of the various effective ΛN central forces [7,16]. In these effective forces, the strength is determined to reproduce the empirical $\Lambda\alpha$ bound-state energy $E_B^{\mathrm{exp}} = -3.12 \pm 0.02$ MeV. On the other hand, Fig. 3 shows the $\Lambda\alpha$ potential, which is obtained from the quark-model baryon-baryon interactions fss2 and FSS [15]. We first calculate the ΛN G-matrix in symmetric nuclear matter, assuming the Fermi momentum, $k_F = 1.35$ fm^{-1}, and the QTQ (qtq) and continuous (cont) choices for intermediate spectra. The $\Lambda\alpha$ Born kernels are then calculated through the α-cluster folding without any approximations. The $\Lambda\alpha$ potential is derived by solving the transcendental equation for the $\Lambda\alpha$ Wigner transform of this $\Lambda\alpha$ Born kernel. The comparison between Figs. 2 and 3 shows that our $\Lambda\alpha$ potential resembles that of the Nijmegen model D simulated potential (ND), and the potential range is rather large. The bound-state energies obtained by solving the Lippmann-Schwinger equation for the $\Lambda\alpha$ Born kernel are -3.62 MeV for fss2 (cont) and -3.18 MeV for FSS (cont). If we assume $k_F = 1.20$ fm^{-1}, we obtain -4.54 MeV for fss2 (cont) and -3.90 MeV for FSS (cont). All these values are lower than the the experimental value -3.12 ± 0.02 MeV, which implies that the central part of our fss2 ΛN interaction is probably slightly too attractive in agreement with the previous finding in the Faddeev calculation of the hypertriton [6].

Another prominent feature of the ΛN interaction is a very small spin-orbit splitting observed in the light Λ hypernuclei. In the non-relativistic description of the ΛN interaction, this feature is usually described by the strong cancellation of the ordinary LS component and the antisymmetric LS ($LS^{(-)}$) component. Since the $\Lambda\alpha$ LS Born

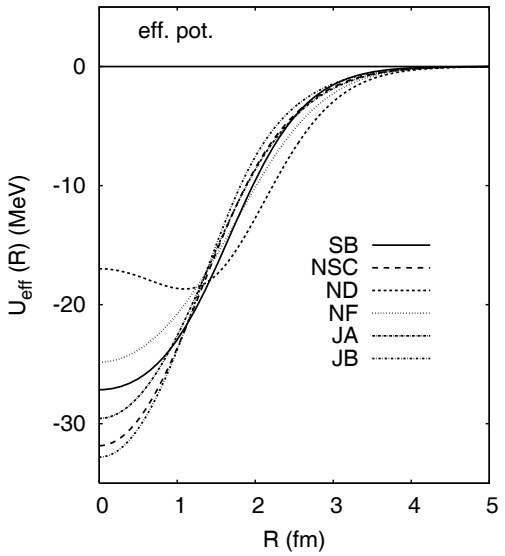

Fig. 2. $\Lambda\alpha$ potentials predicted from the Wigner transform for various effective ΛN potentials: SB (Sparenberg-Baye potential [7]), NSC, ND, NF (simulated versions of the Nijmegen potentials), JA, JB (those of the Jülich potentials) [16]. The energy $E = -3.12$ MeV is assumed.

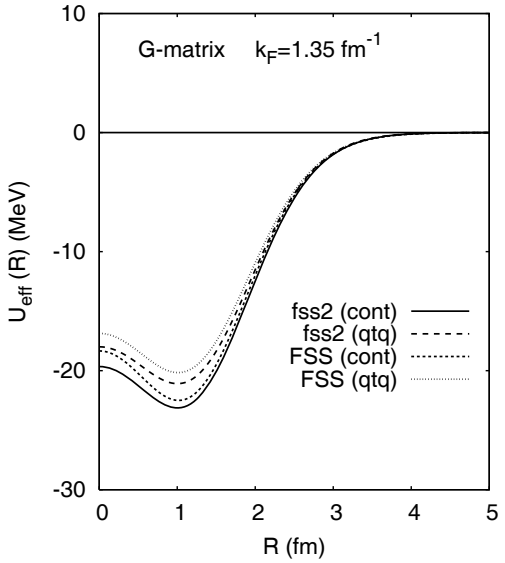

Fig. 3. The same as Fig. 2, but for the Wigner transform calculated from the quark-model G-matrix interactions. The $\Lambda\alpha$ Born kernels are calculated from the quark-model G-matrix B_8B_8 interactions by fss2 and FSS.

kernel is straightforwardly obtained from the ΛN invariant G-matrix, we can use this in the Faddeev calculation of the $\alpha\alpha\Lambda$ three-cluster system [8]. Table 2 lists the results of such Faddeev calculations. The previous results , using the simple folding procedure of the diagonal ΛN Born kernel, and the Scheerbaum factors in symmetric nuclear matter, are also shown. The G-matrix calculation is carried out for three Fermi-momenta, $k_F = 1.07,\ 1.20$, and 1.35 fm^{-1}, which correspond to the densities $\rho = 0.5\rho_0,\ 0.7\rho_0$, and ρ_0, respectively, with ρ_0 being the saturation density. We find that the very small spin-orbit splitting of the ${}^{9}_{\Lambda}$Be excited states [17,18] can be reproduced in the present calculation, using the $\alpha\alpha$ RGM kernel and the $\Lambda\alpha$ LS Born kernel predicted by the FSS G-matrix with $k_F = 1.25$ fm^{-1}. It is noteworthy that the strong cancellation takes place for the Fermi-Breit LS interaction through the important P-wave ΛN–ΣN coupling caused by the $LS^{(-)}$ component. The ℓs splitting is drastically reduced in the ${}^{9}_{\Lambda}$Be system, if a smaller k_F value is used for FSS. On the other hand, the reduction in fss2 is very small, since this model include appreciable LS contribution from the scalar mesons.

Table 2. The ℓs splitting of the ${}^{9}_{\Lambda}$Be excited states by the $\alpha\alpha\Lambda$ Faddeev calculation, using the quark-model G-matrix $\Lambda\alpha$ LS Born kernel. The Scheerbaum factor, S_Λ, in nuclear matter is also listed. The Fermi momenta, $k_F = 1.07,\ 1.20$, and 1.35 fm^{-1} are assumed for the G-matrix calculation by the model fss2 or FSS in the continuous choice for intermediate spectra. "ΛN Born" implies the results obtained when the ΛN single-channel Born kernel is used in S_Λ calculation and the α-cluster folding.

	ρ/ρ_0	0.5	0.7	1	ΛN Born
	k_F (fm^{-1})	1.07	1.20	1.35	–
G-matrix	fss2 (cont)	−10.5	−10.6	−10.7	−10.9
S_Λ (MeV fm^5)	FSS (cont)	−1.9	−2.9	−3.6	−7.8
Faddeev	fss2 (cont)	188	194	198	198
ΔE (keV)	FSS (cont)	7	34	59	137
$\Delta E^{\rm exp}$ (keV)			43 ± 5		

5 $\Sigma\alpha$ and $\Xi\alpha$ potentials

The present formulation using the quark-model G-matrix B_8B_8 interaction is applied to obtain the $\Sigma\alpha$ and $\Xi\alpha$ potentials. When the interaction is repulsive and the square of the local momentum, q^2, becomes negative, the transcendental equation sometimes does not have its solution. Since the extension of the Wigner transform to the negative q^2 is not easy numerically, we only discuss the zero-momentum Wigner transform, $G^C_W(R,0)$, which we call the "$B_8\alpha$ potential" in this subsection. Since these Wigner transforms consist of contributions from two different isospin components for the ΣN and ΞN interactions, it is important to examine each isospin component separately, in order to gain some insight to other possibilities of unknown hypernuclei. Here we discuss some qualitative features of $G^C_W(R,0)$, based on the symmetry properties of the B_8B_8 interactions predicted by the quark-model interactions, FSS and fss2. We focus on the real part of the central potential, which originates from the real part of the central invariant G-matrix interaction.

Figure 4 shows the isospin $I = 1/2$ and $3/2$ contributions to the $\Sigma\alpha$ central potential, predicted by fss2. The results by FSS are qualitatively very similar. We find that the $\Sigma\alpha$ potential has some amount of attraction originat-

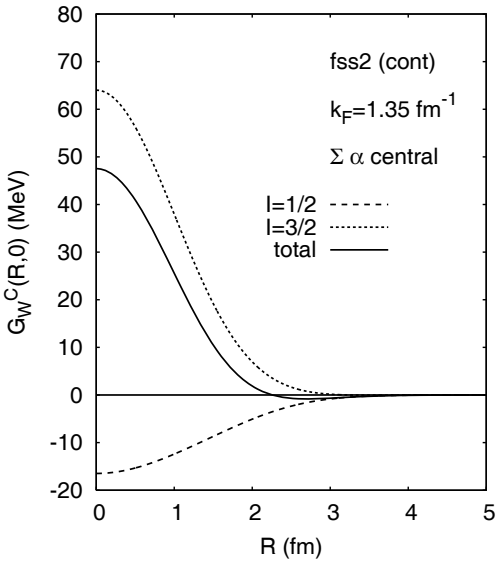

Fig. 4. The central zero-momentum Wigner transform, $G_W^C(R,0)$, for the $\Sigma\alpha$ system, calculated from the quark-model G-matrix B_8B_8 interactions by fss2.

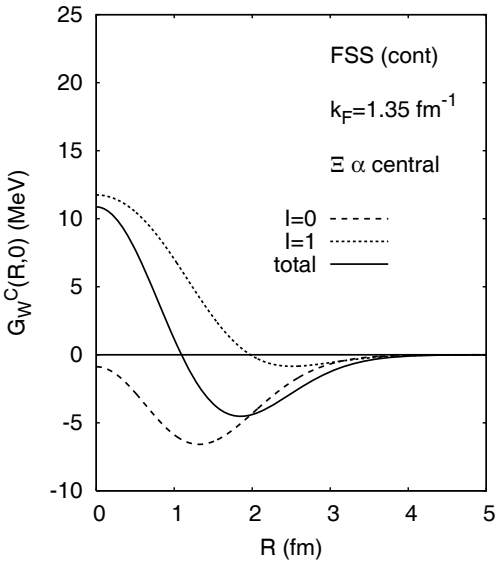

Fig. 5. The same as Fig. 4, but for the $\Xi\alpha$ interaction by FSS.

ing from the $^3S_1$ channel of the $I = 1/2$ ΣN interaction. This channel becomes attractive due to the very strong ΛN–ΣN coupling by the one-pion exchange tensor force. On the other hand, the $^3S_1$ state of the $I = 3/2$ channel is strongly repulsive due to the Pauli principle at the quark level. We find from Fig. 4 that this repulsion is so strong that it makes the $\Sigma\alpha$ interaction repulsive.

Figures 5 and 6 show the $I = 0$ and 1 components for the $\Xi\alpha$ central potential, predicted by FSS and fss2, respectively. Here again we find the situation that the attractive nature of the $I = 0$ component is largely canceled by the repulsion in the $I = 1$ channel. However, this cancellation is not strong especially in the model FSS, and we have almost 5 MeV attraction around $R = 2$ fm. In fss2,

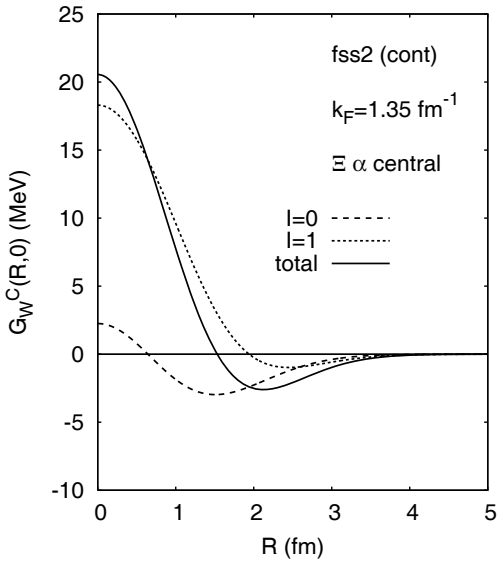

Fig. 6. The same as Fig. 4, but for the $\Xi\alpha$ interaction by fss2.

the height of the central repulsion in the $I = 1$ channel is almost 20 MeV, and we can expect a few MeV attraction in the surface region. These long-range attractions may have some influence on the atomic orbit between Ξ^- and α. It should be noted that the origin of the repulsion in the $I = 1$ channel is the Pauli forbidden state $(11)_s$ in the $^1S_0$ state and the almost Pauli forbidden state (30) in the $^3S_1$ state. However, the coupling with the $\Sigma\Lambda$ channel is very important [2], which may cause the long-range attraction even in the $I = 1$ channel.

6 Λ(3N), Σ(3N) and Ξ(3N) potentials

We have also calculated $B_8(3N)$ potentials, by assuming the $(0s)^3$ $(3N)$-cluster with the h.o. size parameter $\nu = 0.22$ fm^{-2}, which is estimated as an average of $\nu = 0.18$ fm^{-2} for the ^{3}He and ^{3}H clusters and $\nu = 0.257$ fm^{-2} for the α-cluster. The framework developed in Ref. [15] is used by changing the mass number A from 4 to 3. The $B_8(3N)$ Born kernels are calculated from the quark-model G-matrix B_8B_8 interactions by fss2 in the continuous choice for intermediate spectra. The Fermi momentum used in the G-matrix calculation is $k_F = 1.20$ fm^{-1}. Figures 7 and 8 illustrate the zero-momentum Wigner transforms, $G_W(R,0)$, (dashed curves) and the solutions of the transcendental equations (solid curves), obtained from the Born kernels for the $\Lambda(3N)$ $J^\pi = 0^+$ and 1^+ states with $T = 1/2$. The bound state energies of the Lippmann-Schwinger equation, $E_B = -2.06$ MeV for the 0^+ state and -1.02 MeV for the 1^+ state, are used for solving the transcendental equation. These energies are very close to the Λ separation energies, about 2 MeV and 1 MeV of the ${}^4_\Lambda\{\text{He, H}\}(0^+)$ and ${}^4_\Lambda\{\text{He, H}\}(1^+)$ states, respectively. However, these results are rather fortuitous, since more accurate Faddeev-Yakubovsky calculations would yield more binding for the too attractive ΛN interaction of fss2.

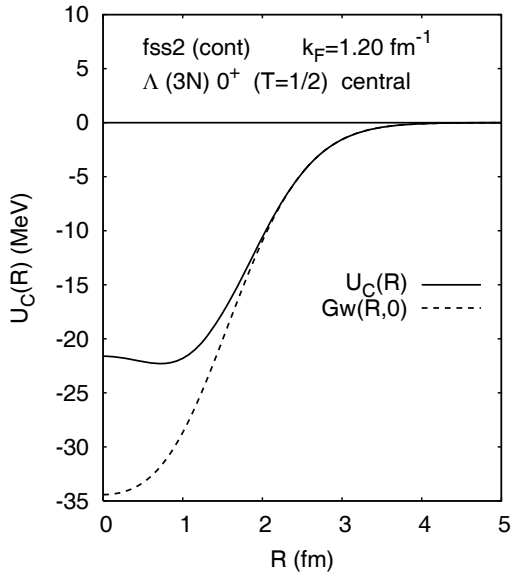

Fig. 7. The zero-momentum Wigner transform (dashed curve) and the solution of the transcendental equation (solid curve), obtained from the Wigner transform of $B_8(3N)$ Born kernels, in the $\Lambda(3N)$ 0^+ state with the isospin $T = 1/2$.

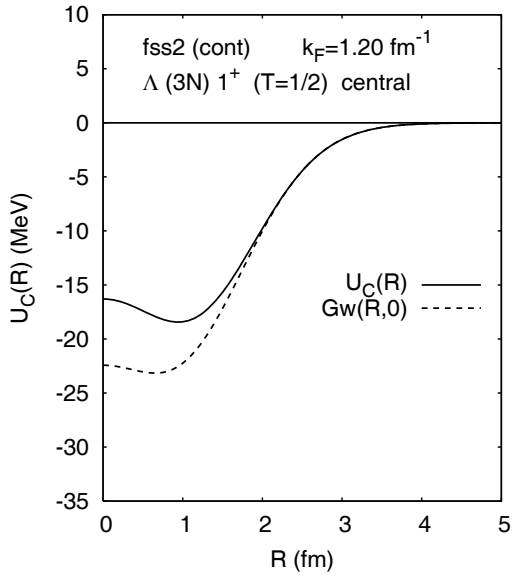

Fig. 8. The same as Fig. 7, but for the 1^+ state.

We find that the $\Sigma(3N)$ potential depicted in Fig. 9 is attractive for the $J^\pi = 0^+$ and $T = 1/2$ state. In this spin-isospin state, the strong repulsion in the $\Sigma N(I = 3/2)\,{}^3S_1$ channel does not contribute. The $\Sigma(3N)$ Born kernel gives the bound-state energy, -7.00 MeV, for $k_F = 1.20$ fm^{-1}, which is a reasonable value for the $\Sigma(3N)$ single-channel calculation. The Σ bound state is observed experimentally in the ${}^4_\Sigma$He(0^+) state with $T = 1/2$, whose binding energy is about 4 MeV and the width is about 7 MeV [19,20]. On the other hand, the $\Xi(3N)$ zero-momentum Wigner transform in Fig. 10 is mostly repulsive in the 0^+ and $T = 0$ channel.

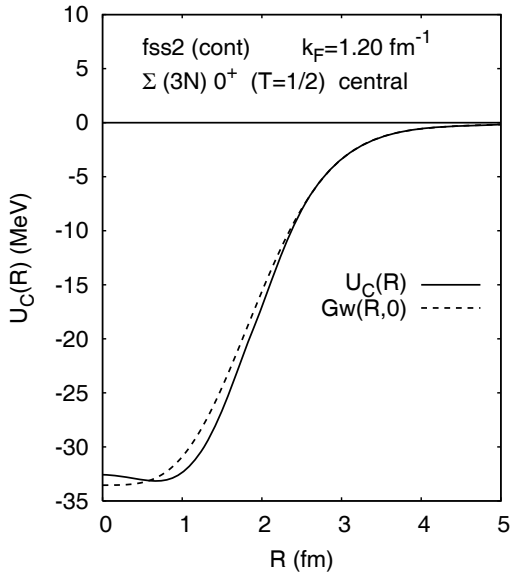

Fig. 9. The same as Fig. 7, but for the $\Sigma(3N)$ 0^+ $(T = 1/2)$ state.

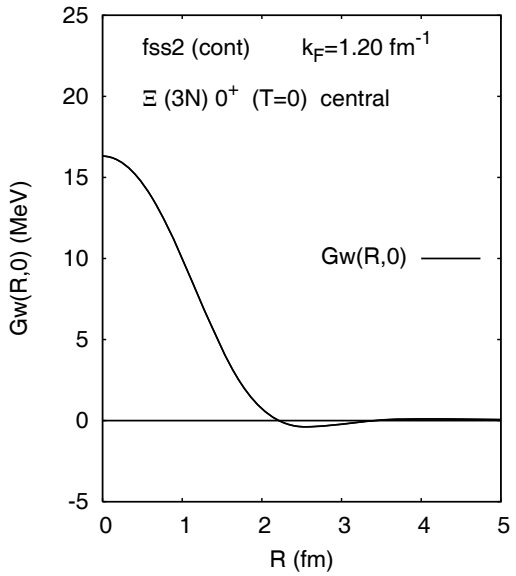

Fig. 10. The zero-momentum Wigner transform for the $\Xi(3N)$ 0^+ $(T = 0)$ state.

7 Ξ^-p and Ξ^0p total cross sections

Figure 11 shows the $\Xi^- p$ and $\Xi^0 p$ total cross sections predicted by FSS (left) and fss2 (right). Both of the isospin $I = 0$ and 1 channels contribute to the $\Xi^- p$ cross sections, while only the channel with $I = 1$ contributes to $\Xi^0 p$ (or $\Xi^- n$). The $\Xi^0 p$ (and $\Xi^- n$) total cross sections with the pure $I = 1$ component are predicted to be very small below the $\Sigma\Lambda$ threshold. This behavior of the $\Xi^- n$ total cross sections is essentially the same as the Nijmegen result [21]. On the other hand, the $\Xi^- p$ total cross sections exhibit a typical channel-coupling behavior which is similar to that of the $\Sigma^- p$ total cross sections. These features demonstrate that the $\Sigma\Lambda$ channel coupling is very important for the correct description of scattering observables,

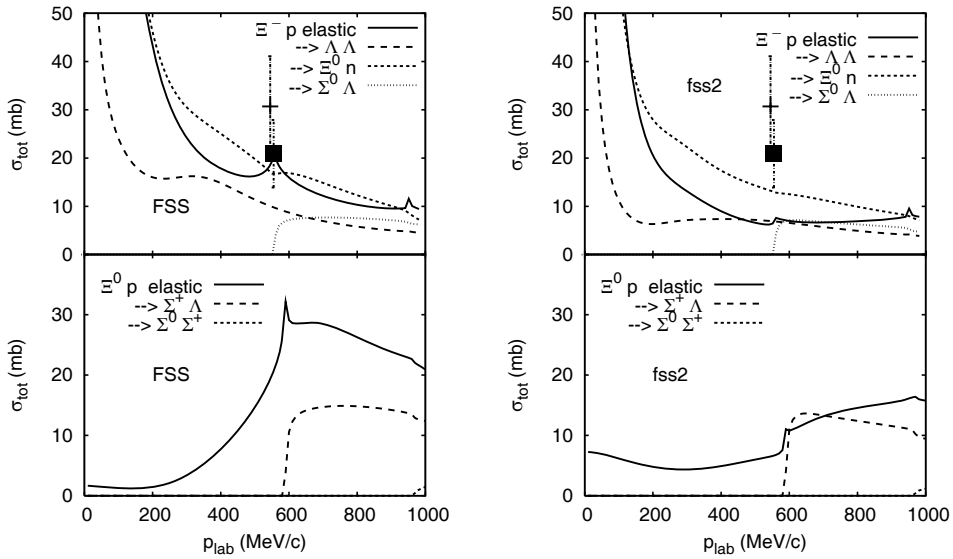

Fig. 11. $\Xi^- p$ and $\Xi^0 p$ total cross sections predicted by FSS (left panels) and fss2 (right panels). The calculation is made in the particle basis, including the pion-Coulomb corrections.

resulting in the strong isospin dependence of the ΞN interaction. Figure 11 also includes the in-medium experimental $\Xi^- N$ total cross section around $p_{\rm lab} = 550$ MeV/c [22], where $\sigma_{\Xi^- N}$ (in medium) $= 30 \pm 6.7^{+3.7}_{-3.6}$ mb is given. Another analysis using the eikonal approximation [23] gives $\sigma = 20.9 \pm 4.5^{+2.5}_{-2.4}$ mb, as shown by the black square in Fig. 11. The analysis also estimates the cross section ratio $\sigma_{\Xi^- p}/\sigma_{\Xi^- n} = 1.1^{+1.4+0.7}_{-0.7-0.4}$ mb. A more recent experimental analysis [24] for the low-energy $\Xi^- p$ elastic and $\Xi^- p \to \Lambda\Lambda$ total cross sections in the range of 0.2 GeV/c to 0.8 GeV/c shows that the former is less than 24 mb at 90% confidence level and the latter of the order of several mb, respectively. These results seem to favor the predictions by fss2. However, we definitely need more experimental data with high statistics.

8 Outlook

The production of Ξ-hypernuclei is scheduled as the Day-1 experiment of the J-PARC project. Rich information on the strangeness $S = -2$ sector will stimulate further theoretical and experimental studies on the strangeness and hypernuclear physics.

This work is supported by Grants-in-Aid for Scientific Research (C) from the Japan Society for the Promotion of Science (JSPS) (Grant Nos. 18540261 and 17540263).

References

1. Y. Fujiwara, Y. Suzuki and C. Nakamoto, Prog. Part. Nucl. Phys. **58**, (2007) 439.
2. Y. Fujiwara, M. Kohno, C. Nakamoto and Y. Suzuki, Phys. Rev. C **64**, 054001 (2001).
3. Y. Fujiwara, T. Fujita, M. Kohno, C. Nakamoto and Y. Suzuki, Phys. Rev. C **65**, 014002 (2002).
4. Y. Fujiwara, K. Miyagawa, M. Kohno, Y. Suzuki and H. Nemura, Phys. Rev. C **66**, 021001 (2002).
5. Y. Fujiwara, K. Miyagawa, Y. Suzuki, M. Kohno and H. Nemura, Nucl. Phys. **A 721**, (2003) 983c.
6. Y. Fujiwara, K. Miyagawa, M. Kohno and Y. Suzuki, Phys. Rev. C **70**, 024001 (2004).
7. Y. Fujiwara, K. Miyagawa, M. Kohno, Y. Suzuki, D. Baye and J.-M. Sparenberg, Phys. Rev. C **70**, 024002 (2004).
8. Y. Fujiwara, M. Kohno, K. Miyagawa and Y. Suzuki, Phys. Rev. C **70**, 047002 (2004).
9. Y. Fujiwara, M. Kohno, K. Miyagawa, Y. Suzuki and J.-M. Sparenberg, Phys. Rev. C **70**, 037001 (2004).
10. Y. Fujiwara, H. Nemura, Y. Suzuki, K. Miyagawa and M. Kohno, Prog. Theor. Phys. **107**, (2002) 745.
11. Y. Fujiwara, Y. Suzuki, K. Miyagawa, M. Kohno and H. Nemura, Prog. Theor. Phys. **107**, (2002) 993.
12. M. Kohno, Y. Fujiwara, T. Fujita, C. Nakamoto and Y. Suzuki, Nucl. Phys. **A 674**, (2000) 229.
13. Y. Fujiwara, M. Kohno, T. Fujita, C. Nakamoto and Y. Suzuki, Nucl. Phys. **A 674**, (2000) 493.
14. M. Kohno, Y. Fujiwara and Y. Akaishi, Phys. Rev. C **68**, 034302 (2003).
15. Y. Fujiwara, M. Kohno and Y. Suzuki, Nucl. Phys. **A 784**, (2007) 161.
16. E. Hiyama, M. Kamimura, T. Motoba, T. Yamada and Y. Yamamoto, Prog. Theor. Phys. **97**, (1997) 881.
17. H. Akikawa *et al.*, Phys. Rev. Lett. **88**, (2002) 082501 .
18. H. Tamura *et al.*, Nucl. Phys. **A 754**, (2005) 58c.
19. R. S. Hayano *et al.*, Phys. Lett. **B 231**, (1989) 355.
20. T. Nagae *et al.*, Phys. Rev. Lett. **80**, (1998)1605.
21. V. G. J. Stoks and Th. A. Rijken, Phys. Rev. C **59**(1999) 3009.
22. T. Tamagawa *et al.*, Nucl. Phys. **A 691**, (2001) 234c.
23. Y. Yamamoto, T. Tamagawa, T. Fukuda and T. Motoba, Prog. Theor. Phys. **106**, (2001) 363.
24. J. K. Ahn *et al.*, Phys. Lett. **B 633**, (2006) 214.